Quantum Study of Information Delay in Electromagnetically Induced Transparency

M. T. L. Hsu,[1] G. Hétet,[1] O. Glöckl,[1] J. J. Longdell,[1,2] B. C. Buchler,[1] H.-A. Bachor,[1] and P. K. Lam[1,*]

[1]*ARC COE for Quantum-Atom Optics, Australian National University, Canberra, ACT 0200, Australia*

[2]*Laser Physics Centre, RSPhysSE, Australian National University, Canberra, ACT 0200, Australia*

(Received 26 June 2006; published 2 November 2006)

Using electromagnetically induced transparency (EIT), it is possible to delay and store light in atomic ensembles. Theoretical modeling and recent experiments have suggested that the EIT storage mechanism can be used as a memory for quantum information. We present experiments that quantify the noise performance of an EIT system for conjugate amplitude and phase quadratures. It is shown that our EIT system adds excess noise to the delayed light that has not hitherto been predicted by published theoretical modeling. In analogy with other continuous-variable quantum information systems, the performance of our EIT system is characterized in terms of conditional variance and signal transfer.

DOI: 10.1103/PhysRevLett.97.183601 PACS numbers: 42.50.Gy, 03.67.−a

Following theoretical proposals [1], electromagnetically induced transparency (EIT) [2] has become the subject of much interest for controlled atomic storage of quantum states of light. Indeed, the delay and storage of optical qubits in an atomic medium via EIT has recently been shown allowing, in principle, the synchronization of quantum information processing systems [3,4]. Earlier works with classical signals in a vapor cell [5] and cold atoms [6] have shown large signal delay with group velocities as low as 17 ms^{-1}. Storage of classical pulses has also been shown for atomic vapor cells [7,8], cold atomic clouds [9], and solid state systems [10,11] (although it should be noted that alternative interpretations of such pulse storage experiments have also been published [12,13]). One experiment [14] has even shown the transmission of a squeezed state through an EIT system in a vapor cell under the conditions of very small delay. While these experiments are all excellent demonstrations of EIT, to the best of our knowledge, no attempt has been made to experimentally quantify the efficacy of EIT for continuous-variable quantum information systems.

Quantum-theoretical treatments of delay and storage via EIT, in the presence of decoherences, have suggested that no excess noise is added to the delayed light [15–18]. These works show that the degradation of a quantum state in an EIT system results from—(i) the finite transparency window and (ii) a degradation in the transparency induced by ground state dephasing. The implication is that, within the EIT window and for small ground state dephasing, quantum states of light can be delayed and preserved in an EIT medium. In this Letter, we present experimental results that examine the quantum noise performance of an EIT system for conjugate amplitude and phase quadratures that are measured at sideband frequencies (ω) around the optical carrier. Since much work on EIT is motivated by quantum information processing, we evaluate the performance of the EIT system using well-established criteria for continuous-variable (CV) quantum state measurements. In analogy with quantum teleportation and nondemolition experiments where states are transferred from an input to an output, we utilize the conditional variance and signal transfer coefficients to quantify the quantum noise properties of our EIT system.

EIT is created by the interaction of probe (E_p) and pump (E_c) fields, in a 3-level Λ-atomic system, as shown in Fig. 1(b). A narrow transparency window is created for the probe beam which, in the absence of the pump, would

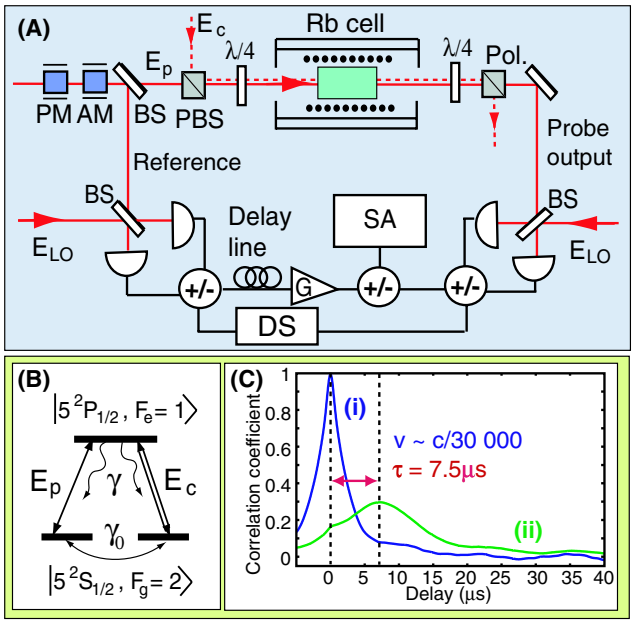

FIG. 1 (color online). (a) Schematic of experimental layout. BS: beam splitter, PBS: polarizing beam splitter, SA: spectrum analyzer, DS: digital storage oscilloscope, $\lambda/4$: quarter-wave plate, $\lambda/2$: half-wave plate, and Pol.: polarizer. (b) Atomic level scheme used in our experiment. E_p is the probe field, E_c is the pump field, γ is the spontaneous emission rate, and γ_0 is the ground state dephasing rate. (c) Amplitude quadrature correlation plots. Similar results were observed for the phase quadrature correlation. Cell temperature = 62 °C; probe and pump power densities are 0.32 mW/cm^2 and 3.2 mW/cm^2, respectively.

be fully absorbed. Solving the optical Bloch equations for the 3-level atomic system, and assuming that $|E_c| \gg |E_p|$, we find a probe susceptibility given by [18,19]

$$\chi(\omega) = \frac{i2N|g|^2(\gamma_0 - i\omega)}{ck[(\gamma_0 - i\omega)(\gamma - i\omega) + |gE_c|^2]}, \quad (1)$$

where k is the wave number, N is the atomic density, g is the atom-field coupling constant, γ is the spontaneous emission rate, and γ_0 is the ground state dephasing rate. The imaginary and real parts of $\chi(\omega)$ describe the transmission and dispersion, respectively, of the probe beam. In particular, on propagation through an EIT medium of length L, the transmissivity of the probe beam is given by $\eta(\omega) = \exp[-\Re\{ik\chi(\omega)L\}]$. This equation describes the transfer of classical probe sideband information at frequency ω through the EIT system, provided the modulation signal is much weaker than the coupling beam mean field amplitude. Under these conditions the EIT system is linear and this equation will also apply to an arbitrary spectrum of sidebands. Note that for $\gamma_0 = 0$ and $\omega = 0$, the EIT system has perfect transmission.

A schematic of our experiment is shown in Fig. 1(a). The experiment was driven using a Ti:sapphire laser, tuned to the $|5^2S_{1/2}, F_g = 2\rangle$ to $|5^2P_{1/2}, F_e = 1\rangle$ transition of the D_1 line of rubidium-87 (^{87}Rb). A beam was encoded with sideband amplitude or phase modulation signals. One half of this beam was sent to a homodyne detection system, as a reference beam for the input. The remainder of this beam was used as a probe, by combining with an orthogonally polarized pump beam at a polarizing beam splitter. The overlapping pump and probe beams were converted to left and right circularly polarized modes by a quarter-wave plate before entering an uncoated, isotopically enhanced ^{87}Rb vapor cell. The heated vapor cell was shielded in two layers of high permeability alloy that reduced stray magnetic fields to ≤ 1 mG. The probe beam was extracted from the output of the cell using a polarizer and sent to a second homodyne detector. The signals from the homodyne detectors were monitored using a digital storage oscilloscope, which was used to obtain time domain data for delay measurements, and a spectrum analyzer, which was used to measure the real-time conditional variance and signal transfer coefficients, in the frequency domain.

The group velocity in an EIT system is typically quantified by measuring the delay of pulses. In our continuous wave system, we applied a 60 kHz bandwidth broadband Gaussian noise modulation to either the amplitude or phase of the probe. By comparing the autocorrelation of the reference beam [Fig. 1(c) (i)] with the cross correlation of the reference and probe output beams [Fig. 1(c) (ii)] we could accurately determine the delay of the amplitude or phase signal. The maximum correlation between the reference and probe output beams occurred at a time delay of 7.5 μs. This corresponded to a group velocity reduction of the input probe beam to $\sim c/30\,000$. The width of curve (ii) is broader than curve (i), indicating that the probe beam has been filtered by the EIT system. Mikhailov *et al.* [20] have reported the spectral narrowing of the modulation width through an EIT medium. This spectral narrowing effect leads to increased correlation times, as shown in Fig. 1(c).

We now analyze the noise performance of our EIT system as a quantum delay line for sidebands at a frequency ω, relative to the carrier frequency of the probe field. This measurement was performed using a spectrum analyzer and broadband Gaussian noise modulation of the amplitude or phase of the probe input beam. Ideally, we would like to possess *a priori* information about the probe input state and then use this information to obtain the conditional variance ($V^{\pm}_{\text{in}|\text{out}}$) between the probe input and output. Without a pair of entangled beams at our disposal, such a direct measurement of $V^{\pm}_{\text{in}|\text{out}}$ is not possible. In practice, we measure the conditional variance between the probe reference and output beams, from which we can infer $V^{\pm}_{\text{in}|\text{out}}$ between probe input and output, as if the beam splitter that separates the probe and reference beams did not exist. The amplitude and phase quadratures are defined in terms of the Fourier transformed annihilation and creation operators, as $\hat{X}^{+}(\omega) = \hat{a}(\omega) + \hat{a}^{\dagger}(\omega)$, and $\hat{X}^{-}(\omega) = i[\hat{a}^{\dagger}(\omega) - \hat{a}(\omega)]$, respectively. The conditional variance is measured by minimizing the subtraction of input and output signals with variable gain $G(\omega)$ and time delay $\tau(\omega)$, giving

$$V^{\pm}_{\text{in}|\text{out}}(\omega) = \min|_{G,\tau}\langle|\hat{X}^{\pm}_{\text{out}}(\omega) - G(\omega)e^{i\omega\tau(\omega)}\hat{X}^{\pm}_{\text{in}}(\omega)|^2\rangle. \quad (2)$$

For an ideal delay line, the conditional variance limit is given by $V^{\pm}_{\text{in}|\text{out}}(\omega) = 0$, since the input and output are exactly equal. A more practical benchmark is an ideal delay line with some inherent passive loss. Equation (1) shows that EIT has frequency dependent transmissivity $\eta(\omega)$. The quantum limit of the conditional variance is therefore found by assuming that this loss is passive, in the sense that transmissivity $\eta(\omega)$ implies the addition of $1 - \eta(\omega)$ units of vacuum noise. In this case the quantum limit of the conditional variance is $V^{\pm}_{\text{in}|\text{out}} = 1 - \eta(\omega)$. Quantum models [18] suggest that EIT systems should reach this passive loss limit, so that an experiment that compares the conditional variance to this quantum limit is a good test of theory. Experimentally, we find the quantum limit by replacing the gas cell with a beam splitter that has the same transmissivity as the EIT system. The transmission of the beam splitter must be adjusted for each sideband frequency to account for the finite EIT transmission [21]. Since $V^{\pm}_{\text{in}|\text{out}}$ for a passive loss is entirely predictable, this "beam splitter benchmark" is also a key indicator that our setup correctly measures $V^{\pm}_{\text{in}|\text{out}}$.

A sample set of $V^{\pm}_{\text{in}|\text{out}}$ data is shown in Fig. 2. The output (i) and reference (ii) signals intersect at a sideband frequency of 305 kHz, corresponding to the frequency at

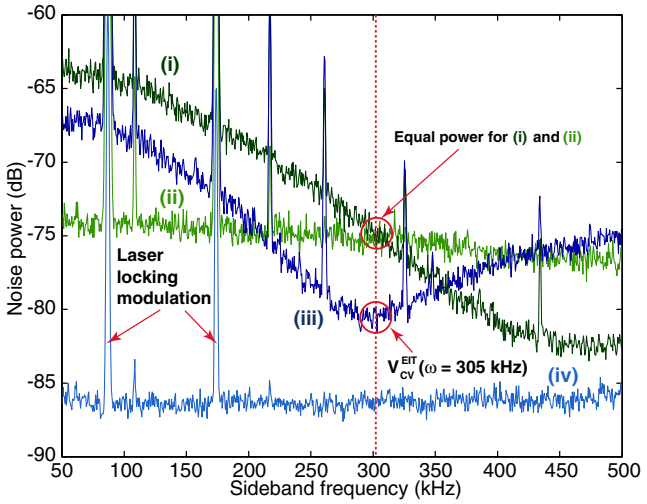

FIG. 2 (color online). $V^{\pm}_{\text{in|out}}$ for the amplitude quadrature, optimized for the sideband frequency of 305 kHz. The curves represent the (i) output probe signal, (ii) reference signal with gain G and delay τ, (iii) $V^{\pm}_{\text{in|out}}$ between the reference and output signals, and (iv) $V^{\pm}_{\text{in|out}}$ for the beam splitter benchmark. The modulation peaks at 87 kHz and 174 kHz are the laser locking signals. Cell temperature = 57 °C; probe and pump power densities are 9.6 mW/cm^2 and 96 mW/cm^2, respectively. Measurements were made with a resolution bandwidth (RBW) = 1 kHz, video bandwidth (VBW) = 30 Hz, and 5 averages.

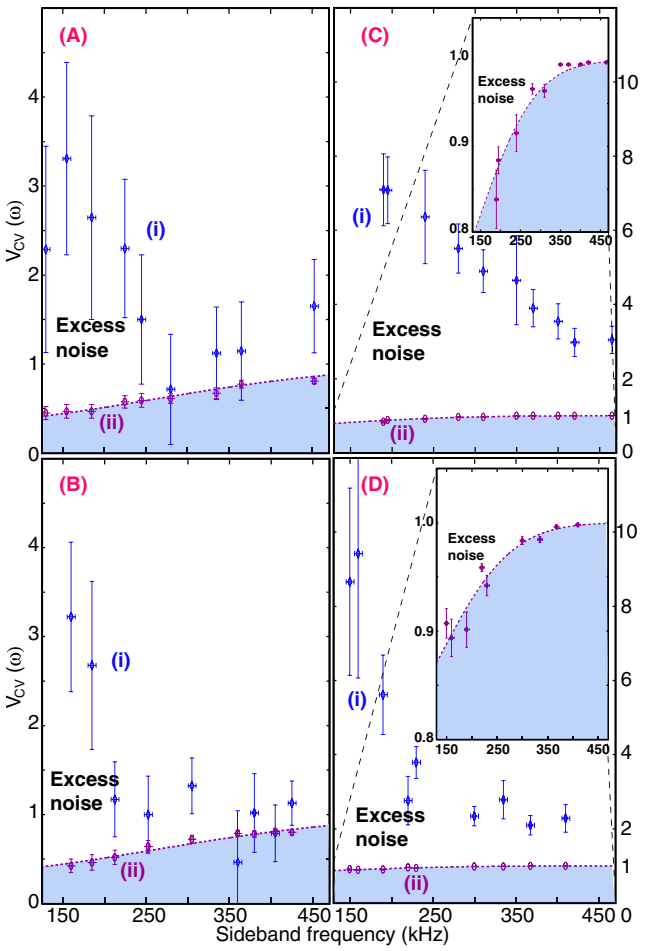

FIG. 3 (color online). $V^{\pm}_{\text{in|out}}$ measurements for 2 cell temperatures. (a) Amplitude quadrature, 42 °C; (b) phase quadrature, 42 °C; (c) amplitude quadrature, 57 °C, and (d) phase quadrature, 57 °C. The data point groups represent the (i) EIT $V^{\pm}_{\text{in|out}}$ and (ii) beam splitter benchmark $V^{\pm}_{\text{in|out}}$. The shape of the shaded area has been fitted using the passive loss described in Eq. (1). The insets show the zoom-in data points. RBW = 1 kHz, VBW = 30 Hz, and 10 averages. The 57 °C and 42 °C beam splitter benchmark data points were fitted with $\gamma_0 = 4$ kHz and $\gamma_0 = 3.5$ kHz, respectively. The probe and pump power densities are 9.6 mW/cm^2 and 96 mW/cm^2, respectively, The largest delay for the 57 °C and 42 °C data is 0.48 μs and 0.18 μs, respectively.

which the $V^{\pm}_{\text{in|out}}$ for the EIT system (iii) is minimum. The $V^{\pm}_{\text{in|out}}$ for the beam splitter benchmark (iv) is lower than the minimum point of curve (iii), indicating that the delayed probe beam has excess noise. Since the EIT system has frequency dependent absorption and delay, the gain and time delay for the $V^{\pm}_{\text{in|out}}$ measurement had to be optimized for each measurement frequency.

Conditional variance results for two different cell temperatures (corresponding to different atomic densities) are shown in Fig. 3. The $V^{\pm}_{\text{in|out}}$ found using a beam splitter to simulate the passive loss of the EIT system are the data sets labeled (ii). Because of the limited bandwidth of EIT, the passive loss increases with sideband frequency so that in the limit of large frequency, the beam splitter reference tends to a value of unity. Using Eq. (1), the EIT window has been fitted to these beam splitter data and is represented by the upper limit of the shaded area. The shaded area therefore indicates the area in which a $V^{\pm}_{\text{in|out}}$ measurement would be exceeding the quantum measurement limit. EIT data (i) are well above the passive loss benchmark (ii), showing that excess noise is added to the delayed probe beam. Moreover, the excess noise is largest at low frequencies where the passive loss benchmark is at its best. For higher sideband frequencies the loss in the EIT system dominates the behavior and $V^{\pm}_{\text{in|out}} \rightarrow 1$.

One source of excess noise is coupling from the pump to the probe [22] since our pump beam has amplitude and phase quadrature noise that lies about 7 dB above the quantum noise limit. By adding amplitude and phase modulation to the pump beam, we were able to measure the transfer functions of the pump-probe coupling. A maximum coupling of 3% for classical phase quadrature signals and 8% for classical amplitude quadrature signals, with negligible levels of cross quadrature coupling, was observed. This is only enough to explain 0.5 dB of excess phase noise and 1.2 dB of excess amplitude noise.

We also quantify the performance of our EIT system in terms of the signal transfer between probe input and output. The signal transfer coefficient is given by $T_s^{\pm}(\omega) = \text{SNR}^{\pm}_{\text{out}}(\omega)/\text{SNR}^{\pm}_{\text{in}}(\omega)$, where $\text{SNR}^{\pm}_{\text{out}}(\omega)$ and $\text{SNR}^{\pm}_{\text{in}}(\omega)$

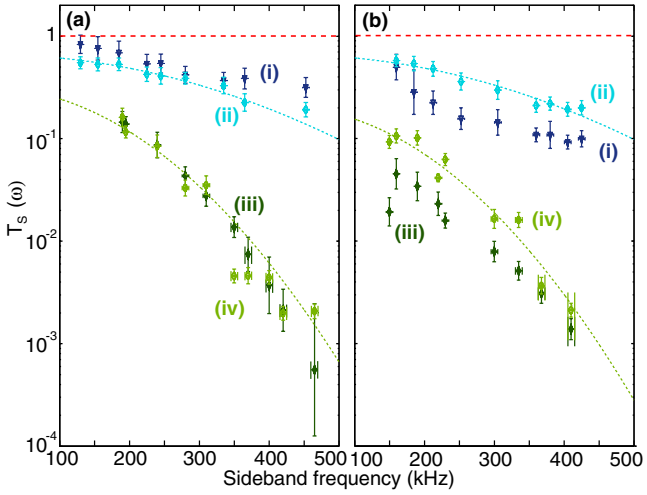

FIG. 4 (color online). Signal transfer coefficient for the (a) amplitude and (b) phase quadratures. (i) $T = 42$ °C and (ii) corresponding beam splitter benchmark. (iii) $T = 57$ °C and (iv) corresponding beam splitter benchmark. RBW = 1 kHz, VBW = 30 Hz, and 10 averages. The probe and pump power densities are 9.6 mW/cm^2 and 96 mW/cm^2, respectively. The 57 °C and 42 °C beam splitter benchmark data points were fitted with $\gamma_0 = 4$ kHz and $\gamma_0 = 3.5$ kHz, respectively.

are the signal-to-noise ratios of the output and input probe fields, respectively. A signal transfer coefficient of unity indicates perfect transfer. This would be the result for a lossless delay line. For a passive system with transmission $\eta(\omega)$, the vacuum noise coupled in by the loss gives a signal transfer of $\eta(\omega)$. Measurements of the signal transfer are shown in Fig. 4. The signal transfer degrades as the frequency increases due to the limited bandwidth of EIT. The EIT system signal transfer is similar to that of the beam splitter benchmark indicating that absorption in the EIT system is the dominant cause of reduced signal transfer. There is some deviation from this behavior for the phase quadrature for both cell temperatures indicating that there is some extra degradation of the phase information.

As discussed above, a deviation of EIT system performance from the passive loss benchmark indicates a discrepancy with the theoretical modeling. Both in terms of conditional variance and signal transfer we see that the EIT system performance measured in our experiment does not reach the passive loss limit. The theoretical modeling [15–18] of EIT does not include several effects. In principle, the pump-probe configuration of EIT means that the experiment is performed on atoms of a particular longitudinal velocity class so that any effects of atomic motion can be ignored. Transverse velocities, however, could play a crucial role. The Gaussian intensity profiles of the pump and probe beams mean that atoms with motion in the transverse plane will experience varying optical field intensities, whereas the theory assumes uniform field intensities. Effects due to high atomic density have also been neglected. Various decoherence mechanisms mean that there is always some fluorescence in the cell. The probability that these photons are reabsorbed by the atoms grows exponentially with atomic density. The quantum noise properties of such "radiation trapping" [23] has not been considered in the context of EIT. Density dependent effects may be of particular interest since they should be more severe in cold atom systems where the density is higher.

In summary, our work shows that light delayed by EIT has significant amounts of excess noise that quantum models of EIT are not yet able to explain. This should serve as a motivation for more complete theoretical models to identify the origins of the noise and also as a caveat to claims that EIT in thermal vapor cells is a good method for storing and delaying quantum states.

The authors thank A. Peng, W. P. Bowen, C. C. Harb, J. J. Hope, and M. Johnsson for fruitful discussions. This work was funded by the ARC Centre of Excellence for Quantum-Atom Optics.

*Email: ping.lam@anu.edu.au

[1] M. Fleischhauer and M. D. Lukin, Phys. Rev. Lett. **84**, 5094 (2000).
[2] K.-J. Boller, A. Imamoglu, and S. E. Harris, Phys. Rev. Lett. **66**, 2593 (1991).
[3] M. D. Eisaman *et al.*, Nature (London) **438**, 837 (2005).
[4] T. Chanelière *et al.*, Nature (London) **438**, 833 (2005).
[5] M. M. Kash *et al.*, Phys. Rev. Lett. **82**, 5229 (1999).
[6] L. V. Hau, S. E. Harris, Z. Dutton, and C. H. Behroozi, Nature (London) **397**, 594 (1999).
[7] D. F. Phillips *et al.*, Phys. Rev. Lett. **86**, 783 (2001).
[8] M. Bajcsy, A. S. Zibrov, and M. D. Lukin, Nature (London) **426**, 638 (2003).
[9] C. Liu, Z. Dutton, C. H. Behroozi, and L. V. Hau, Nature (London) **409**, 490 (2001).
[10] J. J. Longdell, E. Fraval, M. J. Sellars, and N. B. Manson, Phys. Rev. Lett. **95**, 063601 (2005).
[11] A. V. Turukhin *et al.*, Phys. Rev. Lett. **88**, 023602 (2001).
[12] E. B. Alexandrov and V. S. Zapasskii, Phys. Usp. **47**, 1033 (2004).
[13] A. M. Akulshin *et al.*, J. Phys. B **38**, L365 (2005).
[14] D. Akamatsu, K. Akiba, and M. Kozuma, Phys. Rev. Lett. **92**, 203602 (2004).
[15] A. Dantan and M. Pinard, Phys. Rev. A **69**, 043810 (2004).
[16] M. Fleischhauer and M. D. Lukin, Phys. Rev. A **65**, 022314 (2002).
[17] A. B. Matsko *et al.*, Phys. Rev. A **64**, 043809 (2001).
[18] A. Peng *et al.*, Phys. Rev. A **71**, 033809 (2005).
[19] M. O. Scully and M. S. Zubairy, *Quantum Optics* (Cambridge University Press, Cambridge, England, 1997).
[20] E. E. Mikhailov *et al.*, Phys. Rev. A **74**, 013807 (2006).
[21] For probe modulations much larger than the noise added by the EIT medium, $G(\omega) \rightarrow \eta(\omega)$ in Eq. (2). This is how we determined $\eta(\omega)$ independent of the beam splitter used to separate the reference and probe beams.
[22] C. L. G. Alzar *et al.*, Europhys. Lett. **61**, 485 (2003).
[23] A. B. Matsko, I. Novikova, M. O. Scully, and G. R. Welch, Phys. Rev. Lett. **87**, 133601 (2001).